express
polymer letters

Research article

Structure and properties of resole resin crosslinked vulcanizates of natural rubber grafted with polymethylmethacrylate

Nabil Hayeemasae[1,2] *, Siriwat Soontaranon*[3] *, Abdulhakim Masa*[2,4*]

[1]Department of Rubber Technology and Polymer Science, Faculty of Science and Technology, Prince of Songkla University, Pattani Campus, 94000 Pattani, Thailand
[2]Research Unit of Advanced Elastomeric Materials and Innovations for BCG Economy (AEMI), Faculty of Science and Technology, Prince of Songkla University, Pattani Campus, 94000 Pattani, Thailand
[3]Synchrotron Light Research Institute, Muang District, 30000 Nakhon Ratchasima, Thailand
[4]Rubber Engineering and Technology Program, International College, Prince of Songkla University, Hat Yai, 90110 Songkhla, Thailand

Abstract. The structure and property relationships of graft copolymers from natural rubber (NR) and polymethyl methacrylate (PMMA) crosslinked with a phenolic resin were investigated. The NR grafted with PMMA (NR-*g*-PMMA) having different grafting levels was initially prepared by emulsion polymerization before compounding and vulcanization. Then, proton nuclear magnetic resonance and transmission electron microscopy were used to verify the resultant NR-*g*-PMMAs. The graft copolymers crosslinked with phenolic resin exhibited improvements in various properties. Tensile modulus and tensile strength increased at least 18 and 95%, respectively, over the un-grafted counterpart and further improved with grafting percentage, while the elongation at break decreased accordingly. Storage modulus in rubbery plateau increased while tan δ peak height decreased with PMMA content. Moreover, the thermal stability of the graft copolymers was also improved over that of the plain NR at least 23 °C, depending on MMA contents. These improvements are tentatively attributed to the strong adhesion between NR and PMMA phases, based on interactions between the functional groups of PMMA and hydrogen bonding between phenolic resin crosslinker and PMMA. The results clearly suggest that the phenolic resin could be an effective crosslinker for NR-*g*-PMMA.

Keywords: natural rubber, crosslinking agent, vulcanization, grafting, mechanical properties, phenolic resin

1. Introduction

Natural rubber (NR) is considered essential in various engineering applications. Despite its excellent properties, such as high extensibility and tensile strength, NR is also a renewable resource [1]. Due to the high concentration of unsaturated double bonds in its non-polar hydrocarbon structure, NR is readily oxidized when exposed to heat, oxygen, ozone, or light, with poor resistance to oil and heat [2]. Grafting the vinyl monomer such as methyl methacrylate (MMA) onto the NR backbone has proven to be the most effective way to overcome these drawbacks. This copolymer has been commercially available under the trade name Heveaplus MG or as MG rubber [3]. Emulsion polymerization is preferred for producing the graft copolymer because it is more economical and practical than techniques based on a melt or a solution [4]. A remarkable improvement in various properties was observed after NR was grated with PMMA (NR-*g*-PMMA) [5, 6].

Das and Gangopadhyay [7] prepared NR/PMMA blends through interpenetration technique and found that the resultant NR/PMMA blends had a wide range of mechanical properties, depending on the blend compositions. Oommen *et al*. [8] investigated the dynamic mechanical and thermal properties of NR/PMMA blends in the presence and absence of NR-*g*-PMMA as a compatibilizer. The addition of compatibilizer reduces the size of the dispersed phase and increases the storage modulus due to the improved adhesion between the blending components. Moreover, the compatibilized blends were more thermally stable than uncompatibilized blends. Various crosslinking agents have been used to prepare the NR-*g*-PMMA vulcanizates with enhanced properties. Nakason *et al*. [9] investigated the properties of NR-*g*-PMMA crosslinked with sulfur. They found that the NR-*g*-PMMA crosslinked with sulfur exhibited an increasing trend of minimum torque, maximum torque, cure time, and scorch time, affecting the torque difference and crosslink density. The tensile strength of the NR usually increased with the molar fraction of MMA, whereas the elongation at break decreased. Later, Kalkornsurapranee *et al*. [2] investigated using a new type of crosslinking agent, namely glutaraldehyde, for crosslinking NR-*g*-PMMA. The results clearly proved that glutaraldehyde gave an effective curing system. High tensile strength without scarifying extensibility was achieved by curing NR-*g*-PMMA with glutaraldehyde. Moreover, the glutaraldehyde crosslinked NR-*g*-PMMAs still exhibited better mechanical, thermal, and oil-resistance properties than the neat crosslinked NR.

The phenolic resin was found to be another choice to serve as an effective crosslinking agent for NR-based compounds [10–12]. The crosslinked network produced with phenolic resin was more homogenous than that with sulfur [13], and the vulcanizates usually showed excellent heat resistance, low compression set, and good dynamic properties [14]. Therefore, assessing the possibility of using phenolic resin for crosslinking NR-*g*-PMMA is very interesting. The structure-property relationships of phenolic resin crosslinked NR-*g*-PMMA are not well-established. Since the phenolic resin contains hydroxyl (–OH) groups and PMMA contains carbonyl (C=O) groups, strong interactions between phases could prevail in the phenolic resin crosslinked NR-*g*-PMMA. In this study, copolymers of NR and PMMA were prepared by emulsion polymerization. The resultant graft

copolymers were then compounded and compression molded. The successful synthesis of the graft copolymer was confirmed by proton nuclear magnetic resonance and transmission electron microscopy. The tensile properties and microstructure changes, especially in strain-induced crystallization, were investigated using a universal tensile test and wide-angle X-ray scattering (WAXS). The strain-induced crystallization could provide insights into the crystallization mechanisms of NR-*g*-PMMA. The dynamic mechanical and thermal properties were investigated using a dynamic mechanical analyzer and a thermogravimetric analyzer. The possibility of using phenolic resin as a crosslinker for NR-*g*-PMMA is discussed.

2. Materials and methods
2.1. Materials
High ammonium natural rubber latex (HANR) with 60 wt% dry rubber content was supplied by Yala Latex Co., Ltd. (Yala, Thailand). Sodium dodecyl sulfate (SDS), methylmethacrylate (MMA), tetraethylenepentamine (TEPA), and tert-butyl hydroperoxide (TBHPO) were produced by Sigma-Aldrich (Steinheim, Germany). Wingstay-L was manufactured by Eliokem Inc. (Ohio, USA). Resole-type phenolic resin (HRJ-10518) and its catalyst, tin (II) chloride dihydrate (SnCl$_2$·2H$_2$O), were manufactured by Schenectady International Inc. (New Port, USA) and KEMAUS, Elago Enterprises Pty Ltd. (New South Wales, Australia), respectively.

2.2. Preparation of NR-*g*-PMMA
Various NR-*g*-PMMAs were prepared according to the procedure reported by Kalkornsurapranee *et al*. [2]. The NR-*g*-PMMAs were synthesized by emulsion polymerization in the presence of TBHPO and TEPA initiators. The HANR, TEPA, SDS, and deionized water were initially fed into the reactor and stirred at 55 °C under a nitrogen atmosphere. The MMA monomer and TBHPO mixture was then gradually dropped into the reactor via a dropping funnel. The polymerization reaction was performed for 3 h. The variations in NR and MMA are shown in Table 1. Amounts of MMA and 60% HANR are given in dry weight [g], whereas the TBHPO, SDS, and TEPA are given in part(s) per hundred parts of rubber [phr]. The NR-*g*-PMMA samples with different weight ratios of NR and MMA were labeled with NR/MMA 90/10, NR/MMA 80/20, NR/MMA 70/30, and

Table 1. Formulations for preparation of NR-*g*-PMMA.

Ingredient		Dry weight quantities					Delivery
99% MMA	[g]	0	10	20	30	50	Use dropping funnel
80% TBHPO		1.0 phr					
60% HANR latex	[g]	100	90	80	70	50	Place in main reactor
10% SDS		1.5 phr					
85% TEPA		1.0 phr					
Deionized H$_2$O		Adjust TSC to 50%					

NR/MMA 50/50, whereas NR denotes the sample without MMA.

2.3. Compound preparation

The resultant NR-*g*-PMMAs were compounded with other ingredients in an internal mixer, Brabender GmbH & Co. (Duisburg, Germany), at an initial mixing temperature of 40 °C and 60 rpm rotor speed. In this experiment, the temperature was then allowed to increase during mixing until it reached 90 °C at the end of mixing to ensure that the phenolic was melted and well dispersed in the rubber matrix. The list of chemicals is summarized in Table 2. The graft copolymer was first charged into the mixing chamber and masticated for 2 min. The antioxidant was added, and the mixing was continued for 1 min. Next, the HRJ-10518 curing agent was incorporated for 1 min, and the SnCl$_2$·2H$_2$O was finally added. The compounds were discharged from the mixing chamber once the mixing time reached 5 min. The compounds were finally vulcanized by compression molding at 160 °C following their respective curing times.

2.4. Characterization

2.4.1. Transmission electron microscopy (TEM)

The grafted copolymer of NR-*g*-PMMA latex was diluted and stained with osmium tetroxide (OsO$_4$) before subjecting to TEM imaging using JEOL JEM-2010 (JEOL Co., Tokyo, Japan). The accelerating voltage was set at 160 kV.

2.4.2. Proton nuclear magnetic resonance (^{1}H-NMR) analysis

For ^{1}H-NMR spectra, the NR and the various NR-*g*-PMMAs were dissolved in deuterated chloroform (CDCl$_3$) solvent and then characterized by using an Advance Neo 500 MHz NMR spectrometer (Bruker, Rheinstetten, Germany) at room temperature. The mole and weight percentages of PMMA grafted onto the NR were calculated using Equations (1) and (2) [15]:

Mole fraction of PMMA in copolymer [%] =

$$= \frac{I_{3.6/3}}{I_{3.6/3} + I_{5.1}} \cdot 100 \qquad (1)$$

Weight fraction of PMMA in copolymer [%] =

$$= \frac{M_{PMMA} + M_{w_{PMMA}}}{\left(M_{PMMA} + M_{w_{PMMA}}\right) + \left(M_{NR} + M_{w_{NR}}\right)} \qquad (2)$$

where, $I_{3.6}$ and $I_{5.1}$ are the integrals of peak areas at the chemical shifts of 3.6 and 5.1 ppm, respectively. M_{PMMA} and M_{NR} are the molar % fractions of PMMA and NR in the copolymer, and $M_{w_{PMMA}}$ and $M_{w_{NR}}$ are the molecular masses of the repeating units in PMMA (100 g/mol) and NR (68 g/mol), respectively.

2.4.3. Vulcanization property analysis

Vulcanization characteristics, *i.e.*, minimum torque (M_L), maximum torque (M_H), torque difference ($M_H - M_L$), and cure time (t_{90}) of the rubber compounds were measured at 160 °C using a moving die rheometer (MDR 3000 BASIC, Montech, Buchen, Germany).

2.4.4. Swelling equilibrium analysis

The equilibrium swelling test was performed to determine the overall crosslink density (ν) of all

Table 2. Formulations for preparing NR-*g*-PMMA compounds.

Chemical	Quantity [phr]				
	NR	NR/MMA 90/10	NR/MMA 80/20	NR/MMA 70/30	NR/MMA 50/50
NR	100	–	–	–	–
NR/MMA	–	100	100	100	100
Wingstay-L	1	1	1	1	1
HRJ-10518	10	10	10	10	10
SnCl$_2$·2H$_2$O	1	1	1	1	1

vulcanizate samples. The samples were firstly soaked in 30 mL of toluene for 72 h at room temperature. The swollen samples were then wiped and weighed before being de-swollen at 70 °C until their weight remained constant. The ν was were calculated using the Flory-Rehner equation, as shown in Equation (3) [16]:

$$\nu = \frac{\ln(1 - V_r) + V_r + \chi V_r^2}{2\rho V_s(V_r^{1/3} - 0.5V_r)} \cdot 100 \qquad (3)$$

where, χ is the polymer-solvent interaction parameter, ρ is the rubber density, V_s is the molar volume of the solvent and V_r is the volume fraction of rubber in the swollen mass, which can be estimated from Equation (4):

$$V_r = \frac{\frac{W_2}{\rho_r}}{\frac{W_2}{\rho_d} + \frac{W_1 - W_2}{\rho_s}} \qquad (4)$$

where W_2 is the de-swollen weight, W_1 is the swollen weight, ρ_r is the density of rubber, and ρ_s is the density of solvent.

2.4.5. Fourier transform infrared spectroscopic analysis

Fourier-transform infrared (FTIR) spectroscopic analysis of pure NR, pure PMMA, crosslinked NR and crosslinked NR/PMMA were characterized using a Vertex70 (Bruker, Germany). Each spectrum was recorded under attenuated total reflectance (ATR) mode with resolutions of 4 cm^{-1} from 4000 to 400 cm^{-1}. All samples were dried at 70 °C for 3 h before being subjected to the FTIR test.

2.4.6. Tensile property analysis

The dumbbell-shaped samples were cut according to ISO 37 type II. The tensile responses were recorded using a universal tensile testing device, LR5K Plus (Lloyd Instruments, West Sussex, UK). The test was performed at room temperature with a 500 mm/min crosshead speed.

2.4.7. Microstructural analysis

Wide-angle X-ray scattering (WAXS) was used to explore microstructural changes, in particular, the degree of crystallinity during stretching. It was performed at the Siam Photon Laboratory, Synchrotron Light Research Institute, Nakhon Ratchasima, Thailand. The data were recorded during continuous stretching at a 500 mm/min crosshead speed. The SAXSIT data processing program was employed to normalize and rectify all WAXD data.

The crystallinity [%] corresponding to the (200) and (120) planes during stretching was estimated using the Equation (5) [17].

$$\text{Crystallinity [\%]} = \frac{A_c}{A_c + A_a} \cdot 100 \qquad (5)$$

where A_c is the area below the (200) and (120) crystalline peaks and A_a is the area of the amorphous halo.

2.4.8. Dynamic mechanical analysis (DMA)

The dynamic properties of NR/PMMA samples were determined using a dynamic mechanical thermal analyzer, Eplexor 9 (NETZSCH GABO Instrument GmbH, Ahlden, Germany). Measurements were performed over the temperature range from –80 to 80 °C at a heating rate of 2 °C/min and a frequency of 10 Hz in tension mode. The storage modulus and damping factor (tan δ) are reported.

2.4.9. Thermogravimetric analysis (TGA)

The TGA experiments were conducted using a TGA4000 (PerkinElmer, MA, USA) under a nitrogen atmosphere. The testing temperature ranged from 30 to 500 °C with a heating rate of 10 °C/min.

3. Results and discussion
3.1. TEM analysis

Figure 1 depicts the features of a latex particle in neat NR and a representative of the graft copolymer NR/MMA 80/20. The NR latex and the resulting copolymer from NR/MMA were stained with OsO$_4$ vapor to improve the phase contrast between NR and PMMA phases. It is believed that OsO$_4$ can only react with the double bonds in NR molecule chains, causing the NR particles to look dark in TEM micrographs [18]. From Figure 1, it is clear that the nature of the NR particle was spherical in shape with a smooth surface (Figure 1a). In contrast, the grafted NR latex particles had irregularly shaped morphology, with the NR phase surrounded by brighter globular PMMAs (Figure 1b).

The appearance of many globular PMMA particles on the NR particle surface indicates that the grafting of PMMA onto the NR backbone was successful. It is also interesting to observe that unreacted PMMA homopolymers were seen in the copolymer (Figure 1b). Typically, selective extraction of homopolymers from the graft copolymer is used to remove and purify the NR-*g*-PMMA copolymer. Petroleum ether was used
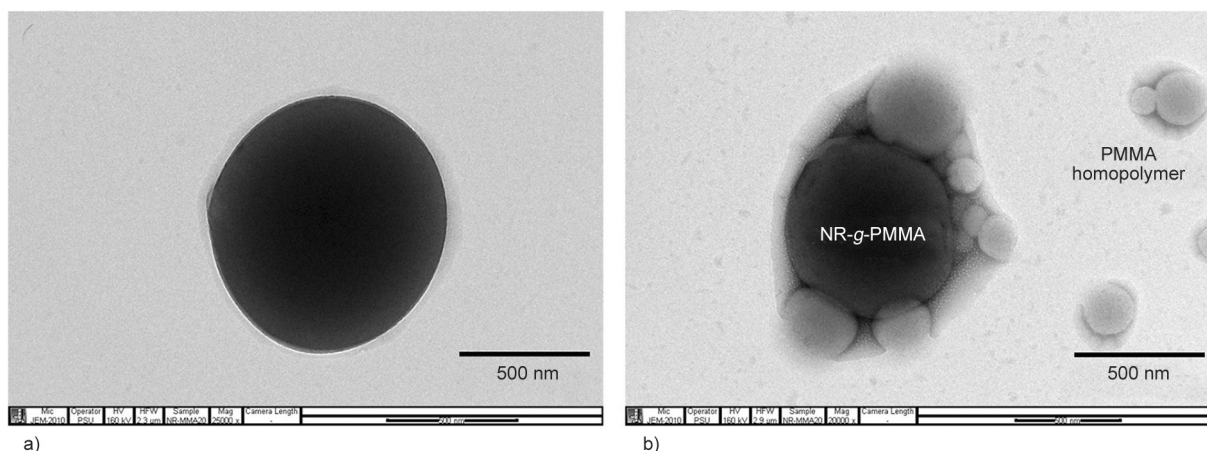
Figure 1. TEM micrographs of representative particles in a) pure NR latex, and b) graft copolymer of NR/MMA 80/20.

to extract the free NR homopolymer (ungrafted NR) and acetone for the free PMMA homopolymer in [2], and the remaining microgels were purified NR-*g*-PMMA products. In this current study, the copolymers were used without further purification. Additional purification may not be practical in production use. In addition, the remaining PMMA homopolymer and MMA monomer may benefit the rubber product due to the extra reactions between functional groups contained in PMMA that could react with the phenolic resin, as will be discussed later.

3.2. ^{1}H-NMR analysis

The product from grafting PMMA onto the NR was further subjected to the ^{1}H-NMR technique using CDCl$_3$ as a solvent. A typical ^{1}H-NMR spectrum of the neat NR and a representative graft copolymer (NR/MMA 50/50) are shown in Figure 2. The characteristic peaks of the NR appeared at 1.7, 2.1, and 5.1 pm, assigned to the protons of –CH$_3$, –CH$_2$, and =CH in the NR [6]. As for the NR-*g*-PMMA, a new absorption peak at the chemical shift of 3.6 ppm was observed, indicating the –OCH$_3$ proton in the PMMA.
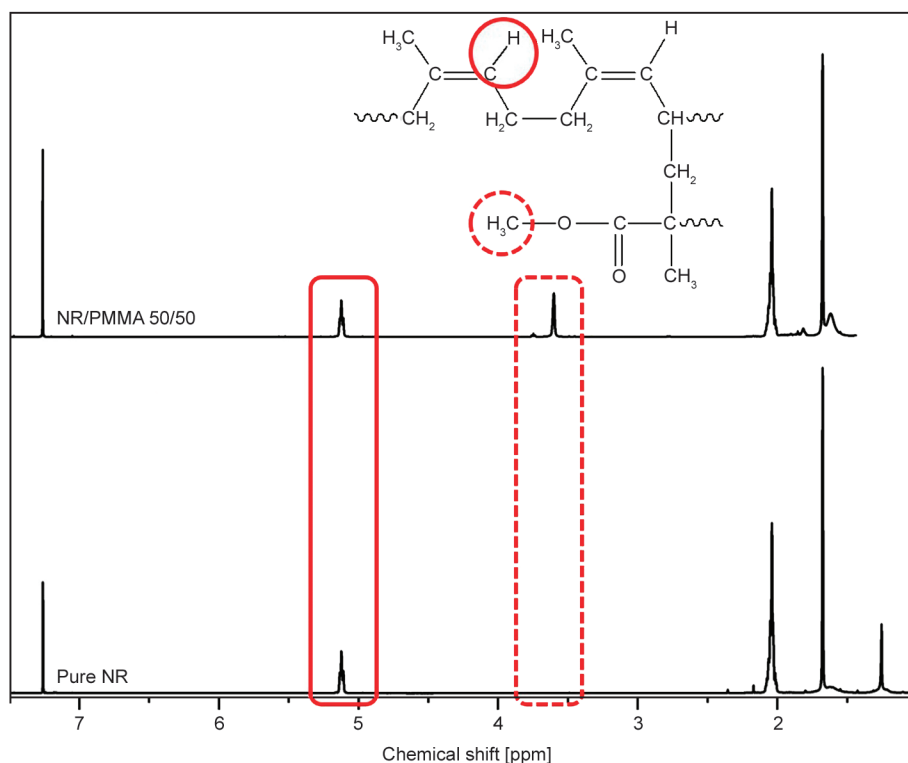
Figure 2. ^{1}H-NMR spectra of NR and of the graft copolymer NR/MMA 50/50.

Table 3. Grafting efficiency at various initial contents of MMA.

Sample name	Initial MMA [wt%]	Grafted PMMA [mol%]	Grafted PMMA [wt%]	Grafting efficiency [%]
NR/MMA 90/10	10	4.5	6.4	64.0
NR/MMA 80/20	20	9.4	13.2	65.0
NR/MMA 70/30	30	14.0	19.4	64.7
NR/MMA 50/50	50	24.8	32.7	65.4

Such a peak clearly confirms the success of grafting PMMA onto the NR. This agrees with prior publications [6, 19, 20].
The integrated peak areas ascribed to the methoxy protons of the grafted PMMA at the chemical shift of 3.6 ppm and the olefinic protons of the NR represented at the 5.1 ppm peak were used to compute the mole and weight percentages of the grafted PMMA on NR, and the results are summarized in Table 3. It can be seen that the amount of grafted PMMA on NR increased with the MMA content provided to the reaction, as expected. The grafting efficiency was about 64–65%, independent of the MMA content. The results clearly suggest that the conditions used to prepare the NR-*g*-PMMA in this study were quite constant. This is in contradiction to many studies showing grafting efficiencies that depended strongly on the content of the monomer used [21, 22].

3.3. Curing properties

Figure 3 shows the vulcanization characteristics of the NR and NR/MMA compounds, while the curing parameters, including M_H, $M_H - M_L$, and t_{90}, are listed in Table 4. Comparing among all samples, increasing MMA content has increased the M_H of vulcanizates, where the highest M_H was seen in the NR/MMA 80/20. This showed that the stiffness of the sample relies on the MMA content, where MMA processes the harder phase. The $M_H - M_L$, an indication of crosslink density, also showed a similar trend. This suggests that the efficiency of the crosslink reaction between NR molecules was reduced when the
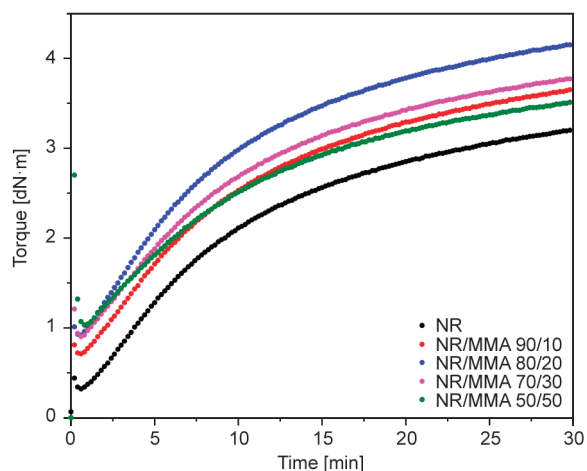
Figure 3. Curing characteristics of the NR and NR/MMA compounds.

MMA content was higher than 20%. The t_{90} of all samples remained more or less constant, suggesting the increased addition of the MMA did not affect the curing time.
The values of ν in various samples measured by the equilibrium swelling test were also included in Table 4. The ν of the graft copolymer increased with increasing MMA contents, revealing the addition of MMA enhanced overall crosslink density of the graft copolymers. As compared to the NR sample, the increase of ν in the NR/MMA samples might be due to the formation of additional interaction between PMMA and phenolic crosslinker. The formation of such interaction was discussed later. It is noted that the crosslink density result obtained from the curing property test and swelling tests showed different trends. This was mainly due to the difference in testing conditions. The curing property was done at high temperatures. Thus, the variation of torque was related to the chemical crosslinks because of the destruction of physical interaction at high temperatures [23]. In contrast, the swelling measurement was conducted at room temperature, where the physical interaction between PMMA and phenolic resin can take place. The acquired overall crosslink density results from the swelling test comprised not only the

Table 4. Maximum torque (M_H), torque differential ($M_H - M_L$), curing time (t_{90}) and crosslink density (ν) of the NR and NR/MMA compounds.

Sample name	M_H [dN·m]	$M_H - M_L$ [dN·m]	t_{90} [min]	ν [mol/cm³]
NR	3.20	2.88	21.51	$3.36\cdot10^{-3}\pm3.88\cdot10^{-5}$
NR/MMA 90/10	3.85	2.93	21.52	$3.67\cdot10^{-3}\pm2.77\cdot10^{-5}$
NR/MMA 80/20	4.16	3.25	21.05	$3.72\cdot10^{-3}\pm1.71\cdot10^{-5}$
NR/MMA 70/30	3.78	2.88	21.36	$3.97\cdot10^{-3}\pm1.30\cdot10^{-5}$
NR/MMA 50/50	3.51	2.48	21.74	$4.52\cdot10^{-3}\pm1.38\cdot10^{-5}$

chemical crosslinks between rubber chains but also the physical crosslinks, *i.e.*, hydrogen bonding between PMMA and phenolic resin and chain entanglements. Therefore, the overall crosslink density of the graft copolymer was increased with MMA content.

3.4. Tensile properties

Figure 4 displays representative stress-strain curves of plain NR and PMMA-grafted NR vulcanizates. The stress-strain patterns of the NR were significantly altered by the incorporation of MMA. Increased MMA content increased the stress at a given strain but decreased the extensibility. The tensile properties in terms of 100 and 300% moduli, tensile strength, and elongation at break are summarized in Table 5. Interestingly, the stress at low strains (100% modulus) and even at high strains (300% modulus) drastically increased with the grafting level of PMMA. The same phenomenon was also found for tensile strength. Despite the enhancement of overall crosslink density, such improvements suggest that strong interfacial interactions were formed in the graft copolymer since weak interfacial adhesion would, in contrast, have degraded the tensile properties [24]. The presence of PMMA increased the interchain interactions between polar functional groups in the graft copolymer, in particular, the carbonyl groups [5]. In addition, the phenolic resin crosslinker contained –OH functional groups, and the PMMA had carbonyl functional groups. Thus, additional interactions were likely formed through hydrogen bonding between PMMA with either grafted PMMA or free PMMA and phenolic resin crosslinker (Figure 5).

The FTIR analysis was performed to confirm the possibility of hydrogen bond formation between PMMA and phenolic resin. Figure 6 reveals FTIR spectra of pure PMMA, pure NR, phenolic resin crosslinked NR, and crosslinked NR/PMMA 80/20 samples. The NR/MMA 80/20 was chosen as a representative of graft copolymer. The main characteristic peaks of the pure PMMA showed at 1725 and
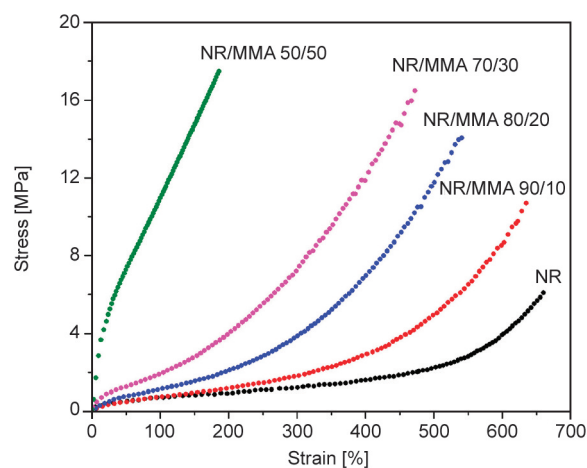
Figure 4. Typical stress-strain curves of NR and graft copolymers of NR and MMA.
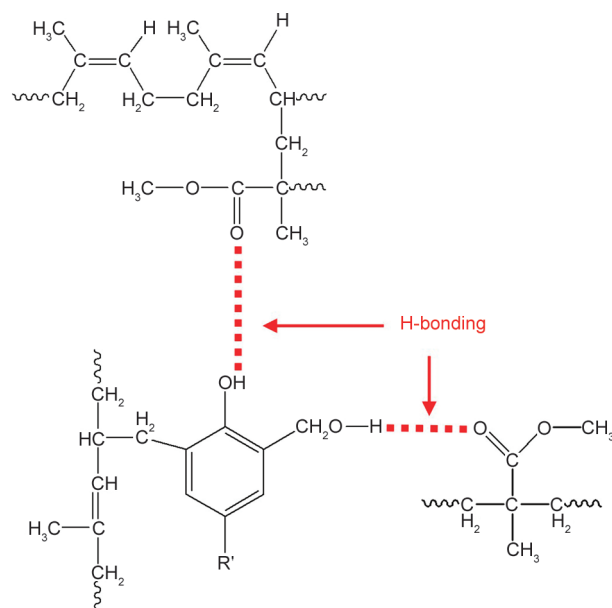
Figure 5. Possible interactions between phenolic resin crosslinker-PMMA (in NR-*g*-PMMA, monomer or homopolymer).

1143 cm^{-1}, corresponding to C=O stretching and C–O stretching vibrations [19]. The pure NR expressed bands at 1663 and 835 cm^{-1}, corresponding to C=C stretching and =C–H out of plane bending, respectively, whereas the phenolic crosslinked NR showed an additional peak centered at 3330 cm^{-1} assigning

Table 5. 100% modulus, 300% modulus, tensile strength and elongation at break of plain NR and of graft copolymers of NR and MMA.

Sample	100% modulus [MPa]	300% modulus [MPa]	Tensile strength [MPa]	Elongation at break [%]
NR	0.62±0.08	1.17±0.08	6.00±0.14	656±8
NR/MMA 90/10	0.73±0.00	1.76±0.01	11.67±0.32	623±40
NR/MMA 80/20	1.17±0.04	3.90±0.24	14.49±0.47	533±20
NR/MMA 70/30	1.91±0.03	7.70±0.37	17.20±0.94	468±31
NR/MMA 50/50	11.74±1.10	N/A	17.99±1.22	180±31
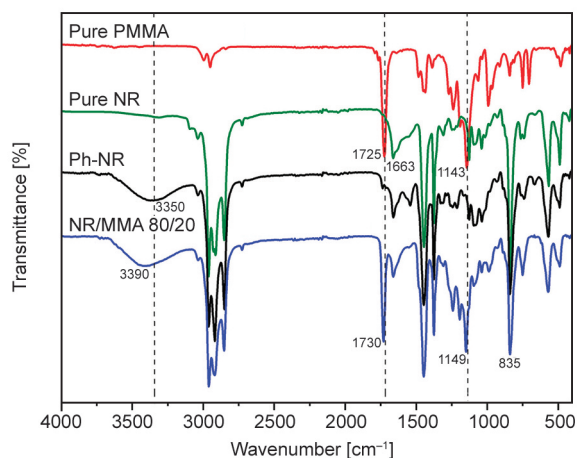
Figure 6. FTIR spectra of pure PMMA, pure NR, phenolic resin crosslinked NR and crosslinked NR/PMMA.

to the –OH vibration of the phenolic resin [11]. All peaks corresponding to pure PMMA, NR, and phenolic resin crosslinked NR were seen in the crosslinked NR/PMMA 80/20. However, it is interesting to mention that the peaks corresponding to C=O, C–O, and –OH were shifted toward a higher wavenumber, *i.e.*, shifted to 1730, 1149, and 3390 cm^{-1}, respectively, after crosslinking the graft copolymer with the phenolic resin. Furthermore, the intensity of peak at 1730 and 1149 cm^{-1} in the crosslinked NR/PMMA 80/20 was also reduced compared to the pure PMMA. This clearly suggests that the C=O, C–O in PMMA, and –OH of phenolic resin in the NR-*g*-PMMA had different chemical environments compared to those of pure PMMA, pure NR, and phenolic resin crosslinked NR. Therefore, the formation of hydrogen bonding between PMMA and phenolic resin, as illustrated in Figure 5, can be confirmed.

The combination of both crosslink density enhancement and hydrogen bonding between crosslinker and PMMA can drastically improve the tensile properties. One may argue that the increased stress was due to the stiffening effect of the PMMA in the rubber matrix. However, since the extensibility of PMMA

is less than 10% [25], the PMMA parts could appear as a weak point, degrading the tensile properties. Only a strong adhesion between NR and PMMA could result in such significant improvements. The variations of tensile properties are in agreement with prior literature [2, 21]. Therefore, the improvements of the tensile modulus and the tensile strength could be the result of good interactions between the NR and MMA. In contrast, the elongation at break of the NR-*g*-PMMAs decreased remarkably due to high interactions between the phases drastically increasing stiffness. A dramatic loss of extensibility was found at a high MMA concentration (NR/MMA 50/50) so less MMA than 50% is suggested for maintaining the flexibility of the copolymer. The values of 100% modulus, 300% modulus, tensile strength, and elongation at break obtained from tensile property measurement were subjected to statistical analysis. The result clearly showed that the properties of graft copolymer were statistically significant and depended on the MMA contents (*P* value < 0.05).

3.5. Strain-induced crystallization behavior
Figure 7 shows 2-dimensional (2D) WAXS images of pure NR and the various NR/MMAs, with the respective strains marked. It is seen that a 2D WAXS image without a reflection spot was observed for the NR sample even at 230% strain, implying that no strain-induced crystallization took place. In contrast, highly oriented crystallite reflection spots were seen, *i.e.*, spots assigned to (200) and (120) planes for the NR/MMA samples. The strain at which the reflection spot was observed shifted toward lower strains in NR-*g*-PMMAs, by an amount dependent on the MMA content, so it was at 235% for NR/MMA 90/10 whereas at 85% for NR/MMA 50/50. The results clearly reveal that the presence of PMMA in the NR facilitated the alignment of NR chains in the stretching direction, accelerating strain-induced crystallization of the NR matrix.
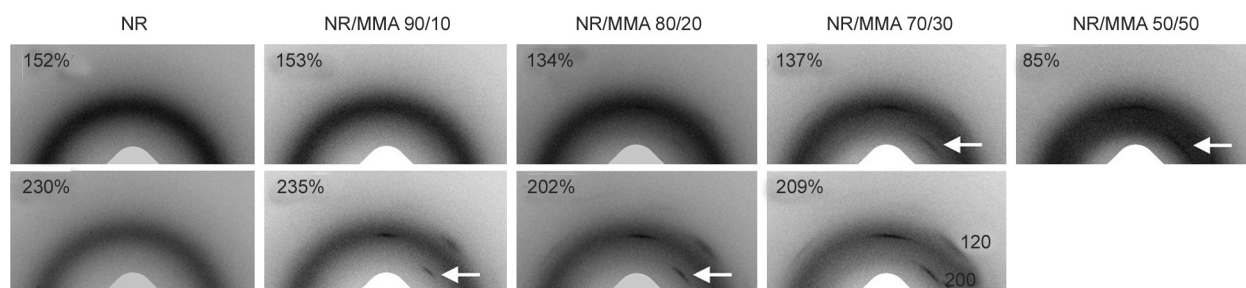
Figure 7. Two-dimensional (2D) WAXS images of NR and of graft copolymers of NR and MMA.
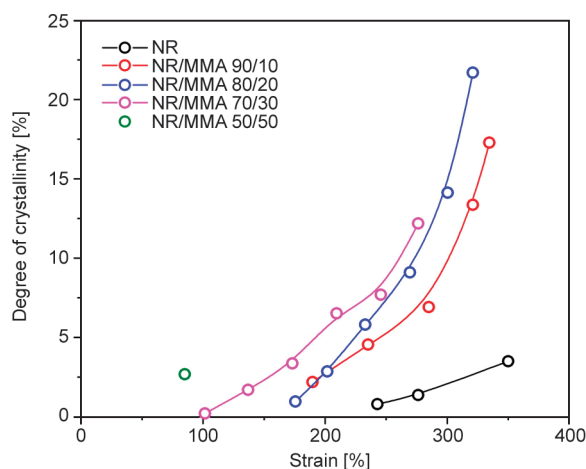
Figure 8. Variation of crystallinity in NR and in graft copolymers of NR and MMA.

The crystallinities of all samples during deformation are shown in Figure 8. It can be seen that the onset of strain-induced crystallinity of phenolic resin crosslinked NR was at about 245%, which is comparable to that in a prior publication [12]. The crystallinity then increased with strain, showing deformation-induced crystallization. Compared to the ungrafted NR, the graft copolymerization induced an earlier onset of crystallization, and the reduction of onset strain tended to get more significant with the percentage of MMA grafted on the NR. The results clearly suggest that the PMMA plays a vital role in speeding up the chain orientation, causing an early strain-induced crystallization. In addition, the PMMA on the NR molecules also increased the overall crystallinity during stretching. Since the extensibility of PMMA is limited (below 10%) [25], PMMA itself would indeed not participate in the crystallization at high strain. It is well accepted that the crystallization

is initiated by the oriented chains or network chains that are highly oriented by stretching [26, 27], thus a large number of short chains could produce a large number of crystal nucleation sites. A reduced onset strain for strain-induced crystallization and an increase in overall crystallinity are likely due to the improved crosslink density, partially resulting from strong interfacial adhesion between NR and PMMA, as previously shown in Figure 5. Such strong adhesion leads to more efficient stress transfer across the rubber matrix. This adhesion increased the number of NR chains that were restricted in mobility, resulting in early rubber chain orientation and hence a lower onset strain for strain-induced crystallization and a higher degree of crystallinity of the NR-*g*-PMMA. Based on this result, the ability for strain-induced crystallization of the NR during stretching could be another approach to assessing the presence of strong interactions between NR and another phase.

3.6. Dynamic mechanical analysis

Figure 9a shows the storage modulus (E') as a function of temperature for NR-*g*-PMMAs. The E' characteristic of ungrafted NR is also included for comparison.

It is seen that increasing the fraction of MMA in the graft copolymer tended to increase E' over the entire temperature range tested. The strong interfacial interactions between rubber and PMMA restricted the molecular mobility of the rubber, and this could be responsible for this observation. Besides the strong interactions between NR and PMMA, an increase in the modulus was also attributed to the high modulus of PMMA domains dispersed in the NR phase, acting as a reinforcing filler in the matrix [28].
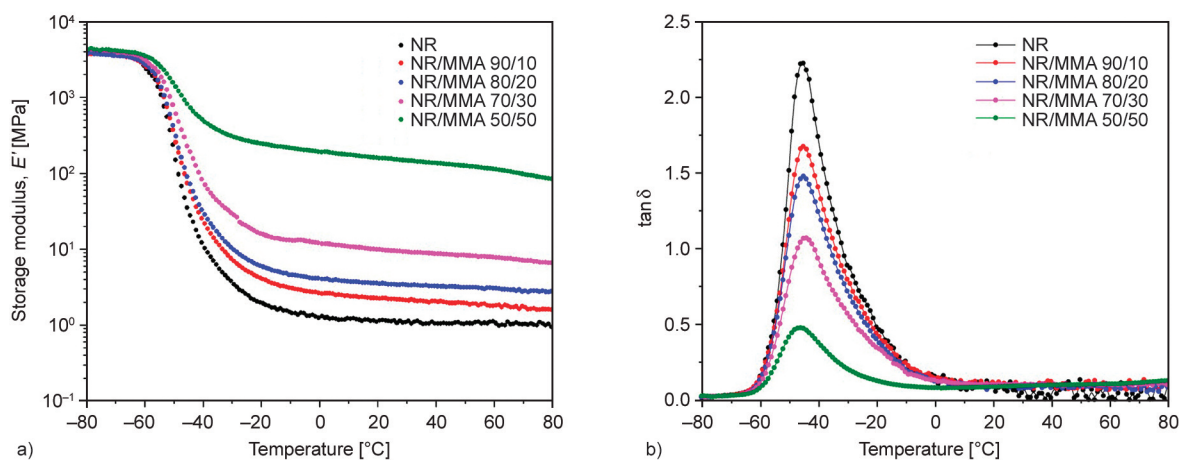
Figure 9. a) Storage modulus, and b) damping factor (tan δ) as functions of temperature for NR and for graft copolymers of NR and MMA.

Figure 9b shows the damping factor (tan δ) as a function of temperature for ungrafted NR and for the graft copolymers containing different NR/MMA ratios. It can be seen that the peak of tan δ, corresponding to the glass transition temperature (T_g), was practically unaffected by the presence of PMMA since the changes in T_g were very small. The T_g of NR was about –46 °C while the NR-*g*-PMMA had about –45 to –47 °C. A drastic change was found in the height of the tan δ, which indicates the chain mobility and damping properties. That is, the tan δ peak height progressively decreased with the MMA content. In the case of rubber composites, a reduction of tan δ peak height usually indicates the presence of filler-matrix interactions. They restrict the mobility of rubber chains, lowering the height of the tan δ peak [29, 30]. Therefore, the decrease in tan δ peak height for NR-*g*-PMMA was attributed to the presence of strong interactions between NR and PMMA phases, by polar-polar interactions and hydrogen bonding between PMMA and phenolic resin cross-linker, as previously discussed. This could effectively limit the mobility of the NR chains, lowering the height of the tan δ peak.

3.7. Thermal properties

Thermal degradation behavior and thermal stability of unmodified- and modified NR were characterized by TGA analysis. Figure 10 shows thermogravimetric curves: (a) weight loss [%], and (b) derivative weight loss versus temperature, for NR and the NR-*g*-PMMAs. It can be seen from Figure 10a that the ungrafted-NR vulcanizate samples showed two regions of degradation. The first degradation was a minor weight loss below 300 °C attributed to the volatile substances, including stearic acid and moisture. Another weight loss step was found at 300–470 °C due to the degradation of rubber molecules [31]. Grafting the PMMA shifted the degradation pattern of the NR toward higher temperatures. The thermal stabilities of all the NR-based samples were evaluated from the temperature at which the sample had lost 5% (T_{d5}) of its initial weight [31].

The T_{d5} of NR was about 285 °C whereas the T_{d5} of NR/MMA 90/10, NR/MMA 80/20, NR/MMA 70/30, and NR/MMA 50/50 were 315, 327, 308 and 317 °C, respectively. The TGA parameters were tabulated in Table 6. The results clearly reveal that the thermal stability of the NR-*g*-PMMAs was greater than that of the NR. This improvement was most likely caused by a higher level of crosslink density and associated loss of unsaturated sites on the NR chains [32, 33]. Besides, additional interactions between the phenolic resin and PMMA cannot be excluded. Since the most significant thermal stability improvement was seen in NR/MMA 80/20, which had about 42 °C greater T_{d5} than the pure one, this may be the best composition for preparing graft copolymer from NR and MMA. Figure 10b shows the derivative weight loss curves of the NR and the NR-*g*-PMMAs. It can be seen that ungrafted NR showed two degradation peaks which were due to volatile substances at below 300 °C and degradation of rubber molecules at above 300 °C. In the case of graft copolymers, the NR-*g*-PMMAs showed three degradation peaks. The first small peak was seen below 300 °C associated with the evaporation of water and bound water in the sample [33]. The second peak was centered at 385–393 °C, depending on the NR/MMA ratio, attributed to the decomposition of rubber chains and the polymeric side
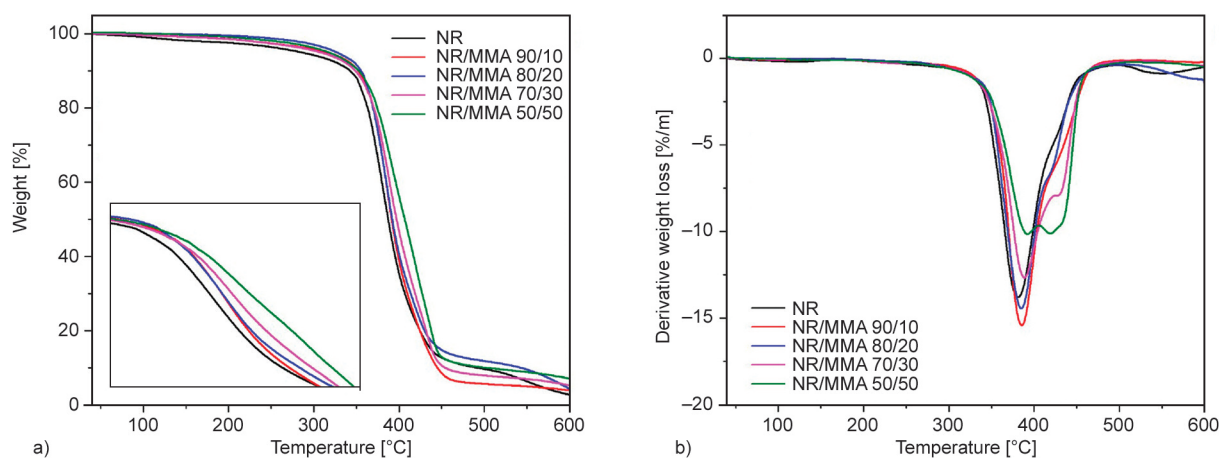
Figure 10. Plot of a) weight loss [%], and b) derivative weight loss versus temperature for NR and for the graft copolymers of NR and MMA.

Table 6. Temperature at which the sample had lost 5% (T_{d5}) of its initial weight, maximum degradation temperature of NR ($T_{dmax\ of\ NR}$) and maximum degradation temperature of PMMA ($T_{dmax\ of\ PMMA}$).

Sample	T_{d5} [°C]	$T_{dmax\ of\ NR}$/degradation rate [°C]/[%/min]	$T_{dmax\ of\ PMMA}$/degradation rate [°C]/[%/min]
NR	285.4	381.1/–13.8	N/A
NR/PMMA 90/10	315.4	385.2/–15.4	N/A
NR/PMMA 80/20	327.1	385.4/14.5	N/A
NR/PMMA 70/30	308.1	388.1/–12.7	429.3/–7.9
NR/PMMA 50/50	317.4	392.5/–10.2	419.0, 432.9/–10.1

chains by the thermal breakage of weaker bonds and terminal groups, such as head-to-head or tail-to-tail bonds in PMMA. The higher peak seen at 419–433 °C was also due to the random scission and depropagation of the PMMA [34]. It is also noticed that the NR-*g*-PMMA exhibited higher decomposition temperature with a lower degradation rate below 400 °C compared to ungrafted NR. Again, this was due to the interactions between the functional groups in the grafted copolymer and the lesser unsaturation of its chains. On the other hand, the increased degradation peak and degradation rate above 400 °C were attributed to a higher amount of PMMA in the graft copolymer.

Based on the results obtained from this study, phenolic resin crosslinked NR-*g*-PMMA provided a significant improvement in various properties including tensile, dynamic, and thermal properties, dependent on the grafting percentage. As a result, there is no doubt that phenolic resin crosslinked NR-*g*-PMMA can be used in several industrial applications.

4. Conclusions

Structure and property relationships for phenolic resin crosslinked graft copolymers of NR and PMMA were investigated. The graft copolymers with different PMMA grafting levels were initially prepared by emulsion polymerization, followed by melt compounding and molding to obtain thin vulcanized sheets. The ^{1}H-NMR and TEM techniques revealed successful preparation of NR-*g*-PMMA graft copolymers. The NR-*g*-PMMAs crosslinked with phenolic resin showed greater tensile strength, dynamic mechanical properties, and thermal stabilities than the plain NR. Such drastic improvement was tentatively attributed to a strong adhesion between NR and PMMA phases. This strength stems from the interactions between the functional groups of PMMA and from hydrogen bonding between phenolic resin crosslinker and PMMA. However, a high grafting level of PMMA, such as in NR/MMA 50/50,

may not be appropriate due to the loss of flexibility and crystallization ability. The best proportions for preparing phenolic resin crosslinked NR-*g*-PMMA have MMA content below 50%. As a result of the high polarity of the MMA and phenolic resin, the phenolic resin crosslinked NR-*g*-PMMA may be promising for utilization as an adhesive and conductive polymer application.

Acknowledgements

References
[1] Roberts A. D.: Natural rubber science and technology. Oxford University Press, New York (1990).

[2] Kalkornsurapranee E., Yung-Aoon W., Thongnuanchan B., Thitithammawong A., Nakason C., Johns J.: Influence of grafting content on the properties of cured natural rubber grafted with PMMAs using glutaraldehyde as a cross-linking agent. Advances in Polymer Technology, **37**, 1478–1485 (2018).
https://doi.org/10.1002/adv.21806

[3] Perera M. C. S., Rowen C. C.: Radiation degradation of MG rubber studied by dynamic mechanical analysis and solid state NMR. Polymer, **41**, 323–334 (2000).
https://doi.org/10.1016/S0032-3861(99)00087-7

[4] Phinyocheep P.: Chemical modification of natural rubber (NR) for improved performance. in 'Chemistry, manufacture and applications of natural rubber' (eds.: Kohjiya S., Ikeda Y.) Woodhead Publishing, Cambridge, 68–118 (2014).
https://doi.org/10.1533/9780857096913.1.68

[5] Saramolee P., Lopattananon N., Sahakaro K.: Preparation and some properties of modified natural rubber bearing grafted poly(methyl methacrylate) and epoxide groups. European Polymer Journal, **56**, 1–10 (2014).
https://doi.org/10.1016/j.eurpolymj.2014.04.008

[6] Kalkornsurapranee E., Sahakaro K., Kaesaman A., Nakason C.: From a laboratory to a pilot scale production of natural rubber grafted with PMMA. Journal of Applied Polymer Science, **114**, 587–597 (2009).
https://doi.org/10.1002/app.30529

[7] Das B., Gangopadhyay T.: Natural rubber-poly(methyl methacrylate) interpenetrating polymer networks – Morphology and mechanical properties. European Polymer Journal, **28**, 867–871 (1992).
https://doi.org/10.1016/0014-3057(92)90312-P

[8] Oommen Z., Groeninckx G., Thomas S.: Dynamic mechanical and thermal properties of physically compatibilized natural rubber/poly(methyl methacrylate) blends by the addition of natural rubber-graft-poly(methyl methacrylate). Journal of Polymer Science Part B: Polymer Physics, **38**, 525–536 (2000).
https://doi.org/10.1002/(SICI)1099-0488(20000215)38:4<525::AID-POLB4>3.0.CO;2-T

[9] Nakason C., Pechurai W., Sahakaro K., Kaesaman A.: Rheological, thermal, and curing properties of natural rubber-*g*-poly(methyl methacrylate). Journal of Applied Polymer Science, **99**, 1600–1614 (2005).
https://doi.org/10.1002/app.22518

[10] Masa A., Iimori S., Saito R., Saito H., Sakai T., Kaesaman A., Lopattananon N.: Strain-induced crystallization behavior of phenolic resin crosslinked natural rubber/clay nanocomposites. Journal of Applied Polymer Science, **132**, 42580 (2015).
https://doi.org/10.1002/app.42580

[11] Masa A., Saito R., Saito H., Sakai T., Kaesaman A., Lopattananon N.: Phenolic resin-crosslinked natural rubber/clay nanocomposites: Influence of clay loading and interfacial adhesion on strain-induced crystallization behavior. Journal of Applied Polymer Science, **133**, 43214 (2016).
https://doi.org/10.1002/app.43214

[12] Hayeemasae N., Soontaranon S., Masa A.: Influence of different vulcanizing agents on structures and properties of sepiolite-filled natural rubber composites. Express Polymer Letters, **17**, 181–195 (2023).
https://doi.org/10.3144/expresspolymlett.2023.13

[13] Osaka N., Kato M., Saito H.: Mechanical properties and network structure of phenol resin crosslinked hydrogenated acrylonitrile-butadiene rubber. Journal of Applied Polymer Science, **129**, 3396–3403 (2013).
https://doi.org/10.1002/app.39010

[14] van Duin M., Souphanthong A.: The chemistry of phenol-formaldehyde resin vulcanization of EPDM: Part I. Evidence for methylene crosslinks. Rubber Chemistry and Technology, **68**, 717–727 (1995).
https://doi.org/10.5254/1.3538768

[15] de Oliveira P. C., de Oliveira A. M., Garcia A., de Souza Barboza J. C., de Cavalho Zavaglia C. A., dos Santos A. M.: Modification of natural rubber: A study by ^{1}H NMR to assess the degree of graftization of polyD-MAEMA or polyMMA onto rubber particles under latex form in the presence of a redox couple initiator. European Polymer Journal, **41**, 1883–1892 (2005).
https://doi.org/10.1016/j.eurpolymj.2005.02.030

[16] Flory P. J., Rehner J.: Statistical mechanics of cross-linked polymer networks I. Rubberlike elasticity. The Journal of Chemical Physics, **11**, 512–520 (1943).
https://doi.org/10.1063/1.1723791

[17] Hernández M., López-Manchado M. A., Sanz A., Nogales A., Ezquerra T. A.: Effects of strain-induced crystallization on the segmental dynamics of vulcanized natural rubber. Macromolecules, **44**, 6574–6580 (2011).
https://doi.org/10.1021/ma201021q

[18] Kangwansupamonkon W., Gilbert R. G., Kiatkamjornwong S.: Modification of natural rubber by grafting with hydrophilic vinyl monomers. Macromolecular Chemistry and Physics, **206**, 2450–2460 (2005).
https://doi.org/10.1002/macp.200500255

[19] Kalkornsurapranee E., Sahakaro K., Kaesaman A., Nakason C.: Influence of reaction volume on the properties of natural rubber-*g*-methyl methacrylate. Journal of Elastomers and Plastics, **42**, 17–34 (2010).
https://doi.org/10.1177/0095244309345410

[20] Promsung R., Nakaramontri Y., Kummerlöwe C., Johns J., Vennemann N., Saetung N., Kalkornsurapranee E.: Grafting of various acrylic monomers on to natural rubber: Effects of glutaraldehyde curing on mechanical and thermo-mechanical properties. Materials Today Communications, **27**, 102387 (2021).
https://doi.org/10.1016/j.mtcomm.2021.102387

[21] Nguyen T. N., Duy H. N., Anh D. T., Thi T. N., Nguyen T. H., Van N. N., Quang T. T., Huy T. N., Thi T. T.: Improvement of thermal and mechanical properties of Vietnam deproteinized natural rubber *via* graft copolymerization with methyl methacrylate. International Journal of Polymer Science, **2020**, 9037827 (2020).
https://doi.org/10.1155/2020/9037827

[22] Thiraphattaraphun L., Kiatkamjornwong S., Prasassarakich P., Damronglerd S.: Natural rubber-*g*-methyl methacrylate/poly(methyl methacrylate) blends. Journal of Applied Polymer Science, **81**, 428–439 (2001).
https://doi.org/10.1002/app.1455

[23] Hayeemasae N., Waesateh K., Soontaranon S., Masa A.: Effect of vulcanization systems and crosslink density on tensile properties and network structures of natural rubber. Jurnal Teknologi, **84**, 181–187 (2022).
https://doi.org/10.11113/jurnalteknologi.v84.16467

[24] Chongprakobkit S., Opaprakasit M., Chuayjuljit S.: Use of PP-*g*-MA prepared by solution process as compatibilizer in polypropylene/polyamide 6 blends. Journal of Metals, Materials and Minerals, **17**, 9–16 (2007).

[25] Wen J.: Poly(methyl acrylate). in 'Polymer data handbook' (ed.: Mark J. E.) Oxford University Press, Oxford, 641–644 (1999).

[26] Tosaka M., Murakami S., Poompradub S., Kohjiya S., Ikeda Y., Toki S., Sics I., Hsiao B. S.: Orientation and crystallization of natural rubber network as revealed by WAXD using synchrotron radiation. Macromolecules, **37**, 3299–3309 (2004).
https://doi.org/10.1021/ma0355608

[27] Kang M. K., Jeon H-J., Song H. H., Kwag G.: Strain-induced crystallization of blends of natural rubber and ultra high cis polybutadiene as studied by synchrotron X-ray diffraction. Macromolecular Research, **24**, 31–36 (2016).
https://doi.org/10.1007/s13233-016-4014-8

[28] John J., Klepac D., Didović M. P., Raju K. V. S. N., Pius A., Andreis M., Srećko V., Thomas S.: Relaxations and chain dynamics of sequential full interpenetrating polymer networks based on natural rubber and poly(methyl methacrylate). Polymer International, **63**, 1427–1438 (2014).
https://doi.org/10.1002/pi.4634

[29] Ikeda Y., Phakkeeree T., Junkong P., Yokohama H., Phinyocheep P., Kitano R., Kato A.: Reinforcing bio-filler 'Lignin' for high performance green natural rubber nanocomposites. RSC Advances, **7**, 5222–5231 (2017).
https://doi.org/10.1039/C6RA26359C

[30] Bashir M. A.: Use of dynamic mechanical analysis (DMA) for characterizing interfacial interactions in filled polymers. Solids, **2**, 108–120 (2021).
https://doi.org/10.3390/solids2010006

[31] Hayeemasae N., Masa A.: Relationship between stress relaxation behavior and thermal stability of natural rubber vulcanizates. Polimeros, **30**, e2020016 (2020).
https://doi.org/10.1590/0104-1428.03120

[32] Zhang C., Man C., Pan Y., Wang W., Jiang L., Dan Y.: Toughening of polylactide with natural rubber grafted with poly(butyl acrylate). Polymer International, **60**, 1548–1555 (2011).
https://doi.org/10.1002/pi.3118

[33] Cui Y., Xiang Y., Xu Y., Wei J., Zhang Z., Li L., Li J.: Poly-acrylic acid grafted natural rubber for multi-coated slow release compound fertilizer: Preparation, properties and slow-release characteristics. International Journal of Biological Macromolecules, **146**, 540–548 (2020).
https://doi.org/10.1016/j.ijbiomac.2020.01.051

[34] Nikolaidis A. K., Achilias D. S.: Thermal degradation kinetics and viscoelastic behavior of poly(methyl methacrylate)/organomodified montmorillonite nanocomposites prepared via in situ bulk radical polymerization. Polymers, **10**, 491 (2018).
https://doi.org/10.3390/polym10050491